EUROPEAN ORGANIZATION FOR NUCLEAR RESEARCH

CERN/EP 84-3
6 January 1984

ASSOCIATED π^0 PRODUCTION IN EVENTS WITH A PARTICLE OF HIGH TRANSVERSE MOMENTUM AT $\sqrt{s}$ = 63 GeV

CERN-Dortmund-Heidelberg-Warsaw Collaboration

K. Doroba[4], D. Drijard[1], H.G. Fischer[1], H. Frehse[1], W. Geist[1], R. Gokieli[4], P. Hanke[3], M. Heiden[1], W. Herr[3], W. Hofmann[2], P.G. Innocenti[1], E.E. Kluge[3], J.W. Lamsa*, T. Lohse[2], W.T. Meyer*, G. Mornacchi[1], T. Nakada[3], M. Panter[1,2], A. Putzer[3], K. Rauschnabel[2], R. Sosnowski[4], J. Spengler[2], O. Ullaland[1] and D. Wegener[2]

1 CERN, European Organization for Nuclear Research, Geneva, Switzerland
2 Institut für Physik der Universität Dortmund, Dortmund, Germany
3 Institut für Hochenergiephysik, Heidelberg, Germany
4 University and Institute for Nuclear Research, Warsaw, Poland
* Visitor from Ames Laboratory and Physics Department, Iowa State University, Ames, USA

ABSTRACT

Events with a single high p_T charged particle were recorded with the Split-Field-Magnet Detector in proton-proton collisions at the CERN-ISR. In the jet opposite to the trigger region the densities of photons and reconstructed neutral pions were measured with a liquid argon shower counter. Scaled momentum distributions of these particles are given and compared with those of charged pions. The spectra of charged and neutral pions coincide. The production cross-section of neutrals in the away jet shows no dependence on the flavour of the trigger particle.

Submitted to Zeitschrift für Physik C

1. INTRODUCTION

Knowledge about the processes yielding particles with high transverse momentum in deep inelastic proton-proton collisions has increased considerably in the last few years [1-6]. Its understanding is based on the parton picture of the proton [7]. Lowest order perturbative QCD describes the scattering amplitude [8], while phenomenological schemes have been quite successful explaining the hadronization of the coloured partons [9].

Experimentally the 4-jet structure of this kind of events is well established [10]: The two transverse jets are formed by the scattered partons, the others by the non-interacting constituents of the protons. The fast leading particle of one of the jets originating from a scattered parton triggers our detector. The requirement of a leading particle in the trigger jet makes it possible to tag the flavour of the parton [11]. The recoil jet, also called the away jet, has no constraints from triggering and is therefore especially suited to study inclusive features of jets.

According to lowest order QCD, which describes the parton scattering successfully, different trigger particles can be related to different scattering processes. For that reason the identification of the flavour of the trigger parton leads on a statistical basis to the knowledge about the away-parton. Therefore it is possible to investigate in the present experiment the fragmentation of different partons into neutral hadrons, which decay to photons. The sample of events was recorded at $\sqrt{s}$ = 63 GeV; the trigger particle has a mean transverse momentum $\langle p_T \rangle$ = 4.7 GeV/c.

2. EXPERIMENTAL SET-UP

The experiment was performed at the CERN ISR using the upgraded Split-Field-Magnet Detector (SFM) [12], which allows the measurement of the momenta of charged particles in almost 4π steradians. The experimental set-up and the special features of the system used to trigger on charged particles with high momenta are described elsewhere [4].

The analysis presented in this paper is based on the data obtained with a shower detector opposite the trigger telescopes (fig. 1). It will be described here briefly, for more details see ref. [13].

2.1 The Liquid-Argon Shower Counter

This detector was a liquid argon shower counter of 16.5 χ^{o} centered at 90° with respect to the line of flight of the colliding protons and an azimuthal angle of ϕ = 180° with respect to the trigger. Its acceptance covered ±0.3 units of rapidity and ±6° of ϕ. Its distance from the vertex was 4.8 m.

The sensitive region of the detector consisted of five identical modules. They were stacks of 1 mm thick lead sheets, separated by a gap of 4 mm. These stacks were aligned along the y-axis (ISR-coordinate-system, see fig. 1) in a vessel filled with liquid argon.

The lead sheets were alternately at high-voltage and ground potential and formed a series of ionization chambers along the depth of a module. To gain spatial resolution, the sheets at high-voltage, which were read out, were divided into strips each 6 cm wide. The orientation of the strips parallel to the y or z direction alternated along the x-axis. To minimize the amount of cable passing from the liquid argon vessel to the exterior and the amount of electronics, several strips were grouped together to form channels directly at the module. The way this was done can be seen in fig. 2, which shows a top and a side view of one module. The continuous lines indicate the regions actually read out as single channels. These regions were designed so as to optimize the identification of electromagnetic showers. Their main signature is the way they deposit energy in the longitudinal direction. For energies as measured in our experiment (<4 GeV) the characteristic maximum can be found within the first six radiation lengths. Therefore a successful identification requires a good resolution in this part of the shower.

For the calculation of the invariant mass of two photons, the distance between their intersection points with the detector is needed to determine their opening angle. Therefore these points of intersection were measured with the maximal resolution, i.e. the width of a strip.

Directly at the module, the signal was decoupled from the high voltage with a capacitor and outside the cryostat fed into a charge-sensitive preamplifier [14]. Then the pulses were shaped and transmitted via twisted pairs to the control room, where a receiver-amplifier shaped them such that an Analog to Digital Converter (LeCroy 2249) could digitize them.

2.2 The Calibration of the Shower Counter

The calibration of the detector was done in three steps. For details see ref. [13]. The first step was the calibration of the electronics. To do this, pulses of known charge were injected into the electronic chain at preamplifier level. The electronics was linear and stable over the whole period of running time.

For the relative calibration of the detector , the signals of minimum ionizing particles were used. They controlled three parameters on which the calibration might depend. The first is the place inside the detector where energy was deposited. Within statistical errors no dependence was found; the detector was homogeneous to better than 5%. Two effects which might reduce the charge seen by the electronics, were corrected by one global calibration constant. It takes into account possible losses on the cables between the stacks and the preamplifiers and corrects for the losses of ionization electrons due to electronegative contamination in the liquid argon. 32% of the charge expected by simple calculation of the energy loss of minimum ionizing particles was collected. Neglecting losses on cables, this number corresponds to an oxygen content of 4-5 ppm [15]. During the period of data taking (3 months) this value was constant to within 2%.

The mass of the π^0-meson was used for the absolute calibration of the detector. After applying a correction for leakage at the back of the detector and for the about 5% of dead areas, a calculation using the Monte-Carlo program EGS [16] confirmed to better than 5% the calibration with the π^0-mass.

3. PARTICLE IDENTIFICATION

3.1 γ Identification

The pattern recognition in the shower detector was split into three steps. At first tracks were searched for in the counter itself. Secondly tracks of charged particles, determined in the proportional chambers, were extrapolated to the front plane of the shower counter and, if possible, combined with a measurement there. As the third step electromagnetic showers were identified by the longitudinal development of their energy deposition.

For the pattern recognition in the shower counter only channels with a charge content of more than three times the r.m.s. of the noise distribution were used. This is equivalent to a charge of less than half the deposit of a minimum ionizing particle. A track candidate was a cluster of hits in one projection along a straight line roughly pointing to the event vertex. Track candidates from the two different projections were combined to a track in space if their length and energy were compatible.

In the second step tracks of charged particles found by the proportional chambers were extrapolated to the shower detector. They were combined with signals of this counter if the distance between the extrapolation and the measured coordinates was less than 10 cm. This value was determined by calculating all possible distances and looking for the correlation peak. By the same method the number of accidental combinations was estimated to be 5%.

To identify electromagnetic showers the ratio R of the energy deposited in the last two planes of channels divided by that of the second plane was used. According to the EGS-Monte-Carlo this ratio R is about 1 for shower energies between 0.2 and 2 GeV/c. For particles with constant energy loss like minimum ionizing particles, R is 3. If R versus energy deposit is plotted, the electromagnetic showers are clearly visible and completely separated from minimum ionizing particles. From this plot the background due to hadronic showers was estimated by extrapolating from a region where neither electromagnetic showers nor minimum ionizing particles enter to be less than 0.5% [13].

3.2 π^0 Reconstruction

Using all electromagnetic showers found by the procedure described above, the invariant mass of two photons was calculated under the assumption that the decay vertex coincided with the event vertex. This is valid for all π^0 mesons which are not daughters of decaying K mesons. A clear π^0 signal can be seen in the $\gamma\gamma$-mass distribution in fig. 3. The background was determined by combining photons from different events and has been subtracted. The variance of 18.5±2.1 MeV/c^2 reflects the resolution of the detector. In the sample of tracks not identified as electromagnetic showers no indication for a π^0 peak was found.

4. MONTE-CARLO SIMULATION

The results obtained with the shower detector were interpreted with the help of a Monte-Carlo program, which simulates the π^0 or η decay and the acceptance and resolution of the detector.

Neutral particles were generated according to the p_T, y and ϕ distribution of charged pions and their two-photon decays simulated. As for real data the detection and identification of the photons were simulated. Then the $\gamma\gamma$ mass was calculated. The systematic errors introduced by simplifying details in the detector and analysis procedure are estimated to be in the order of 10 to 15%.

The broken line in fig. 3 shows the expectation of this Monte-Carlo program for the mass distribution of π^0 mesons. The agreement with the data is very good.

In the same way it is easy to show that no signal from η decays can be seen. Assuming that $\sigma(\eta)/\sigma(\pi^0) = 0.5$ [17] and $\sigma(\pi^0) = (\sigma(\pi^+)+\sigma(\pi^-))/2$, 5 reconstructable η mesons can be expected for the integrated luminosity of our experiment. The distribution of the invariant mass in the region of the η mass is compatible with this number (90% confidence level).

5. RESULTS

5.1 Pseudotrigger

It is important to be sure that the measured photons were produced in the fragmentation process of the parton scattered off the trigger parton, in other words, that they belong to the away jet.

The Monte-Carlo program explained above suggests that about 85% of all photons are decay products from mesons of the away jet. The 15% left are mainly products of η or ω decays in the spectator regions.

To verify experimentally this prediction, the method of pseudo-triggers was applied [10]. The idea is to look for a jet with a leading particle. This particle carries most of the momentum of the scattered parton and thereby defines to a high degree the jet axis. For such jets it is easy to show that the other particles belonging to the jet, cluster around its leading particle.

For our data it was proven that photons follow a charged leading particle or that charged particles follow a leading neutral particle. The number of particles following the pseudotrigger confirm the expectation that 85% of the photons belong to the away jet [13]. This result is within the statistical errors independent of cuts in the transverse momentum.

5.2 The Number of Pions in the Away Jet

The next step was to determine the particle density of π^0 produced in the away jet in order to compare it with the corresponding density of charged pions. This was done for pions with a momentum in the laboratory system higher than 1.2 GeV/c. For purely geometrical reasons, the acceptance for π^0-mesons is approximately independent of their momenta above this limit. In addition this limit is equivalent to a cut in the transverse momentum, which assures that the background of π^0 mesons originating from the spectators is negligible. The number of fully reconstructed π^0 mesons is 232±22. Multiplied by the acceptance

determined by Monte-Carlo, the away jet contains 11,220±1,070 π^0 mesons, compared to 21,650±150 $\pi^{\pm}$. The ratio of charged to neutral pions is therefore

$$\frac{\sigma(\pi^+ + \pi^-)}{\sigma(\pi^0)} = 1.93 \pm 0.18$$

In addition a systematic error of 15% due to the acceptance corrections must be taken into account. This result is in agreement with isospin symmetry.

5.3 The Number of Photons

With the help of the Monte-Carlo program described above the number of photons in the acceptance of the shower counter was estimated. The result is shown in table I for all photons and for the subsample with an energy larger than 1 GeV. The decay products of π^0 mesons are estimated under the assumption of isospin symmetry.

The contributions of the 2 γ decay of the η meson and the π^0-γ decay of the ω -- only the γ is taken into account -- were obtained by assuming $\eta/\pi^0 = 0.5$ [17] and $\omega/\pi^0 = 1$ [18]. These ratios were as well successfully used in fragmentation-models [9]. The numbers of photons from η and ω decays are lower limits because only their contribution from the away jet was considered. Because of the high Q-value, decay products of η and ω mesons produced in the fragmentation of the spectator partons contribute to the number of photons in the away jet region.

The number of photons produced in kaon decays is the most difficult to determine. In K-decays where π^0 mesons were produced, the two photons were generated between the event vertex and the shower detector and often they were still too close together in space to be detected separately.

The calculated numbers quoted in table I are within errors compatible with the measured numbers of photons. They confirm the result obtained with fully reconstructed π^0 mesons that isospin symmetry holds in the fragmentation of the away jet.

5.4 x_E Distributions

To look in a more detailed way for differences in the production of $\pi^{\pm}$ and π^{o}, their x_E distributions are compared. x_E gives the transverse momentum of a particle $\vec{p}_T$ projected and normalized on the $\vec{p}_T(t)$ of the trigger particle $x_E = \vec{p}_T \cdot \vec{p}_T(t) / |\vec{p}_T(t)|^2$. The trigger particle carries as a leading particle on average 75-80% of the momentum of the trigger jet [19]. The transverse momentum of the trigger jet is in first approximation balanced by the away jet. x_E is therefore a good variable to describe the fragmentation of the away jet [10].

Fig. 4a shows the x_E distributions of the $\pi^{\pm}$ and π^{o} mesons. Both are acceptance corrected. It can be seen that the slopes of the two distributions are compatible within the statistical uncertainties. There is no indication of different production mechanisms for $\pi^{\pm}$ and π^{o} mesons.

Because of the much higher statistics for single photons it is worthwhile trying to confirm the result derived from the π^{o}-sample. The x_E distribution of γ originating from the 2 γ decays is a convolution of the x_E distribution of the mother particle and the way its energy is shared between the daughters. The full dots in fig. 4b show the x_E distribution of charged pions. The line gives a parametrization of the data.

The broken line is the result of convoluting the x_E distribution of $\pi^{\pm}$ with an isotropic two photon decay. This curve fits well the measured x_E-distribution of the photons. We can conclude therefore that the x_E distribution of particles which decay into photons (π^{o},η,...) are close to that of the charged pions. It should be noted that the mass of the decaying particle practically does not enter the convolution. So there is no difference in photons originating from π^{o}- or η-mesons observable.

5.5 Comparison of Different Triggers

It is of great interest to see whether the density or the momentum distribution of the photons produced in the away jet show any dependence on the flavour of the triggering particle. This could be the case, if the

following picture holds: π^+, K^+ and π^-, which have a valence quark in common with the proton, are more likely leading particles of quark jets, while the K^- trigger particle should come dominantly from a gluon jet [11]. Under the assumption that in the range of Q^2 values investigated, quark-gluon scattering is the dominant subprocess, the triggers on π^+, K^+ and π^- enrich gluon jets on the away side, and the K^- triggers enrich quark jets [20].

In order to look for differences in the composition of quark and gluon jets, three ways of analysing the data were used [13].

The photon multiplicity in the away jet, the x_E distribution and the ratio of photons over charged particles are investigated as a function of the triggering particle. The number of events with n photons (n = 1,2,3) shows no dependence on the flavour of the trigger. One would expect a correlation, if the η/π^0 ratio would be different for quark and gluon jets, since the probability of detecting both photons from a π^0 in the shower counter is much higher than detecting both from a η decay.

Differences in the x_E distribution should reveal photons with a momentum distribution different to those produced in two photon decays or different x_E distributions of their parents. Within the statistical uncertainties, all x_E distributions are alike.

The ratio $\gamma/\pi^{\pm}$ shows that the away jet contains a fixed fraction of neutrals independently of the flavour of the trigger particle.

6. CONCLUSIONS

We measured the density of photons in the region of phase space opposite to a trigger requiring a particle of high transverse momentum. They are generated in the fragmentation of the parton scattered against the trigger parton. The x_E distribution of reconstructed π^0-mesons is compatible in shape and normalization with that of π^+ and π^--mesons. The x_E distribution of all photons measured confirms this result.

It is expected that K^- triggers enrich quark jets on the away side, while π^+, π^- and K^+ triggers enrich gluon jets. Studies of the γ and π^o content of the away jets for different types of trigger particles show that there is no visible difference between the two types of jets in their content of photons.

Acknowledgements

We are especially grateful for the support provided by the SFM detector group and the ISR experimental support group. We thank J. Engler, H. Keim and the Karlsruhe team for the conception and their contribution to the construction of the liquid argon shower counter. The Dortmund and Heidelberg groups were supported by a grant from the Bundesministerium für Wissenschaft und Forschung of the Federal Republic of Germany. The Dortmund group was also supported by the Ministerium für Wissenschaft und Forschung des Landes Nordrhein - Westfalen.

REFERENCES

[1] D. Drijard et al., Nucl. Phys. B156 (1979) 309;
J. Eichmeyer et al., Phys. Rev. Lett. 46 (1981) 398.

[2] D. Drijard et al., Phys. Lett. 121B (1983) 433.

[3] A.L.S. Angelis et al., CERN/EP 82-133.

[4] D. Drijard et al., Nucl. Phys. B208 (1082) 1.

[5] R.P. Feynman et al., Phys. Rev. D18 (1978) 3320.

[6] R.D. Field, Phys. Rev. D27 (1983) 546.

[7] J.D. Bjorken, E.A. Paschos, Phys. Rev. 185 (1969) 1975.

[8] R. Cutler, D. Sivers, Phys. Rev. D16 (1977) 679, D17 (1978) 196;
B.L. Combridge et al., Phys. Lett. 70B (1977) 234;
J.F. Owens et al., Phys. Rev. D18 (1978) 1501.

[9] B. Andersson et al., Z. Phys. C1 (1979) 105;
R.P. Feynman, R.D. Fields, Nucl. Phys. B136 (1978) 1.

[10] M. Della Negra et al., Nucl. Phys. B127 (1977) 1;
A. Breakstone et al., The Jet Structure of Large Transverse Momentum Events in pp-Interactions, submitted to the XXI International Conference on High Energy Physics, 26-31 July 1982, Paris and to be published.

[11] A. Breakstone et al., High p_T K^--Mesons as Leading Fragments of Gluon Jets in Hard pp-Interactions, (to be published);
A. Breakstone et al., High p_T Hadrons as Leading Particles in Jets at the ISR, (to be published).

[12] R. Bouclier et al., Nucl. Instr. and Meth. 115 (1974) 235;
R. Bouclier et al., Nucl. Instr. and Meth. 125 (1975) 19;
W. Bell et al., Nucl. Instr. and Meth. 156 (1978) 111.

[13] M. Panter, Dissertation Dortmund (1982).

[14] V. Radeka, IEEE Trans. Nucl. Sci., NS21, nr.1 (1974) 51.

[15] L.S. Miller, S. Howe, W.E. Spear, Phys. Rev. 166 (1968) 871.
W. Hofmann et al., Nucl. Instr. and Meth. 135 (1976) 151.

[16] R.L. Ford, W.R. Nelson, SLAC-210, UC-32 (1978).

[17] F.W. Büsser et al., Phys. Lett. B55 (1975) 232;
G.J. Donaldson et al., Phys. Rev. Lett. 40 (1978) 684;
C. Kourkoumelis et al, Phys. Lett. 84B (1979) 271.

[18] M. Diakonou et al, Phys. Lett. 89B (1980) 432.

[19] C.D. Buchanan, presented at the XVIIth Rencontre de Moriond, Les Arcs, 20-26 March 1982.

[20] M. Glück, E. Reya, Phys. Lett. 98B (1981) 444.

TABLE 1

Estimation of the number of photons originating from different decays compared with the data

	γ	γ (E > 1 GeV)
π^0	5580	1250
$\eta \rightarrow \gamma\gamma$	> 2180	> 510
$\omega \rightarrow \pi^0\gamma$	> 650	> 140
$K+, K-, K_L^0$	~ 670	~ 150
Total	> 9080	>2050
Data	10050	2369

FIGURE CAPTIONS

Fig. 1 The Split-Field-Magnet detector at the CERN-ISR: Top view showing the layout of multiwire proportional chambers and the external apparatus for particle identification.

Fig. 2 Top view and side view of one of the modules of the liquid argon shower counter.

Fig. 3 The π^o signal in the invariant mass of photons. The background is subtracted. The broken line shows a Monte-Carlo simulation.

Fig. 4 The x_E distribution of reconstructed π^o mesons (a) and photons (b) in comparison with the distribution of charged pions.

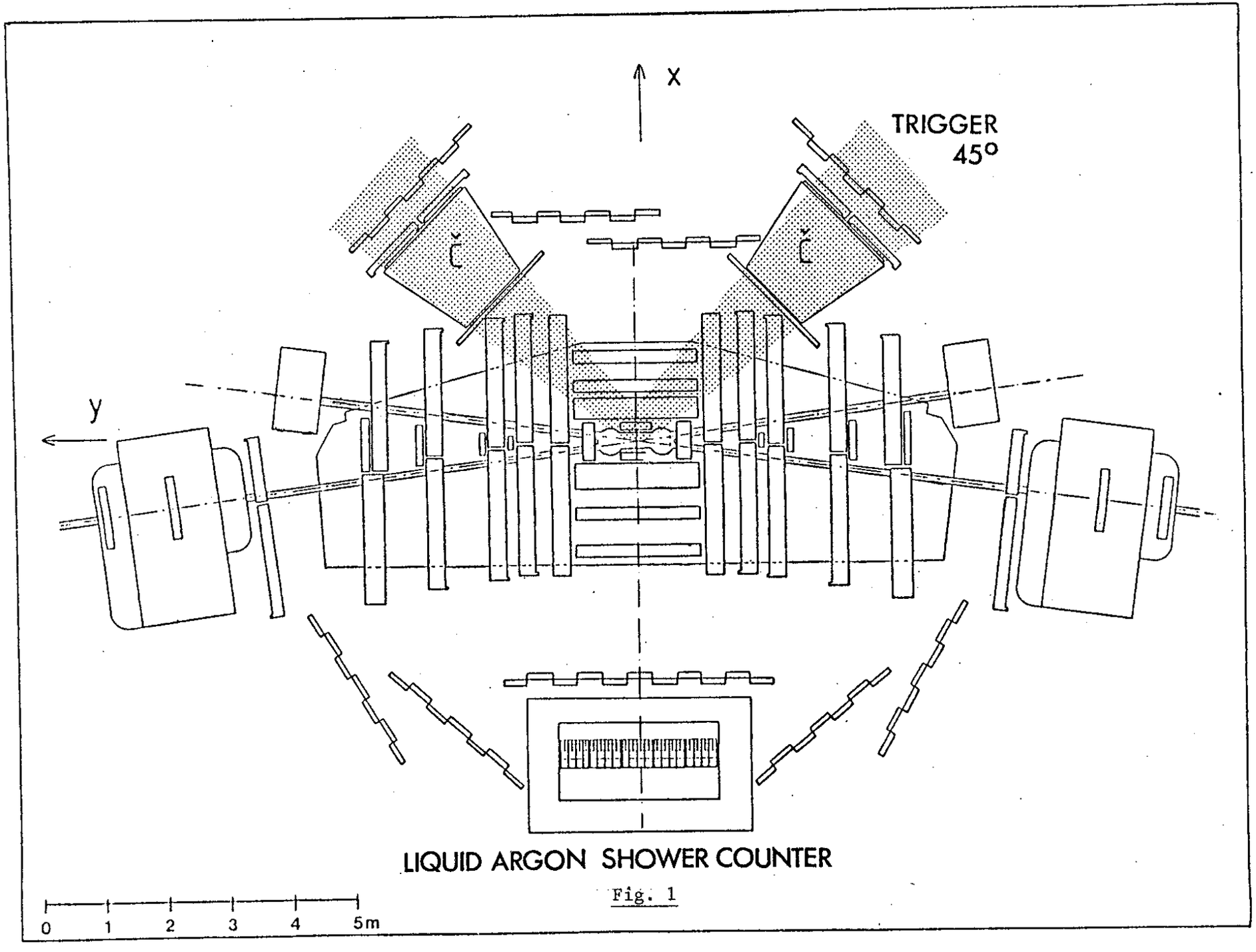

Fig. 1

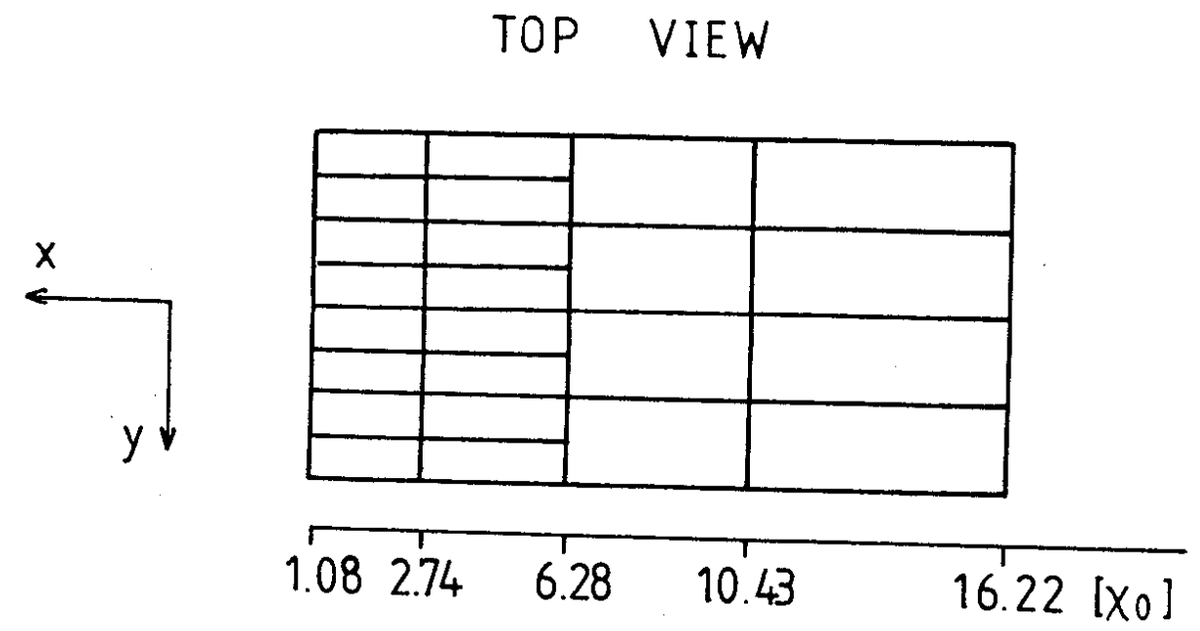
TOP VIEW
x
y
1.08
2.74
6.28
10.43
16.22 [X0]

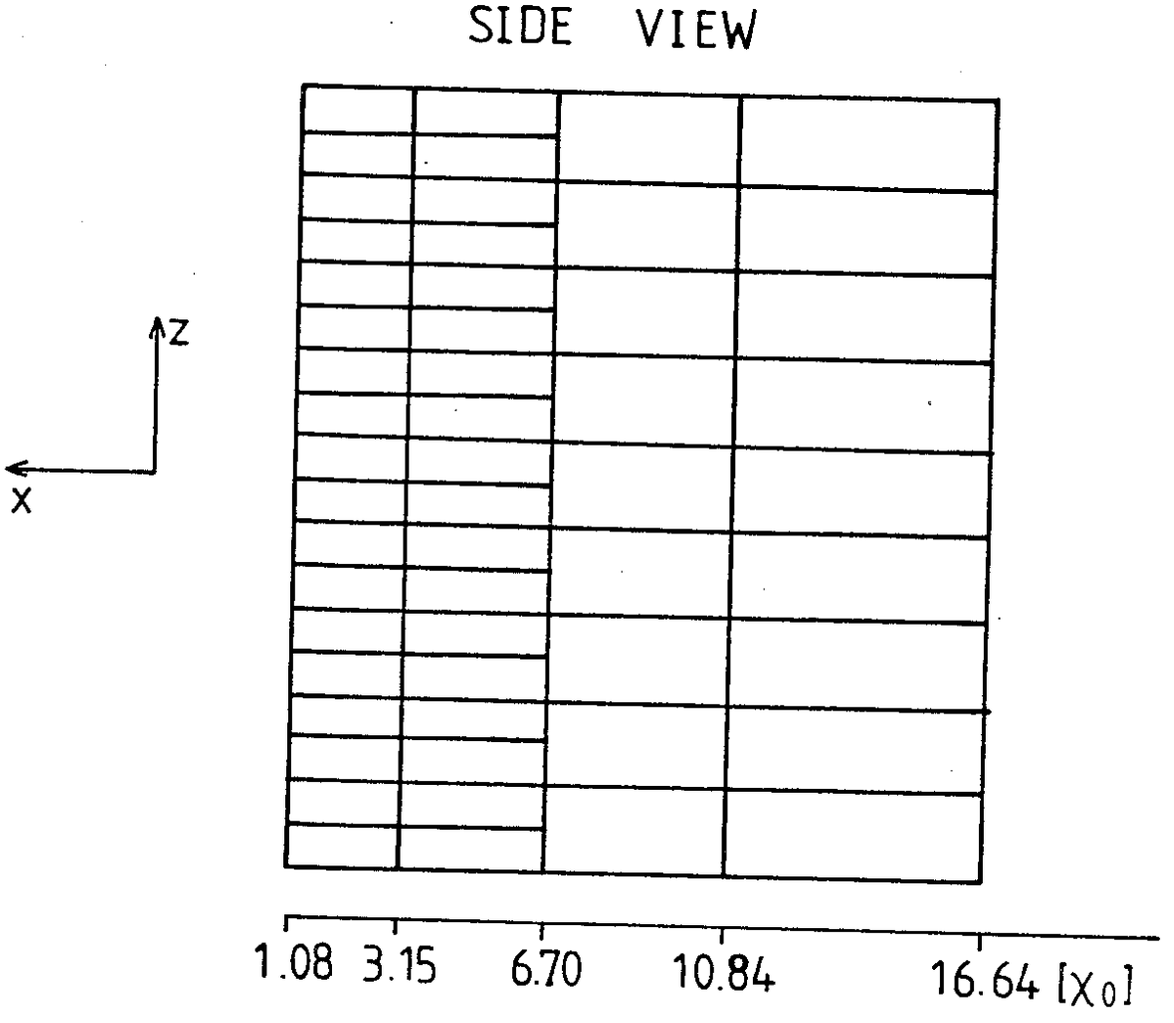
SIDE VIEW
z
x
1.08
3.15
6.70
10.84
16.64 [X0]

Fig. 2

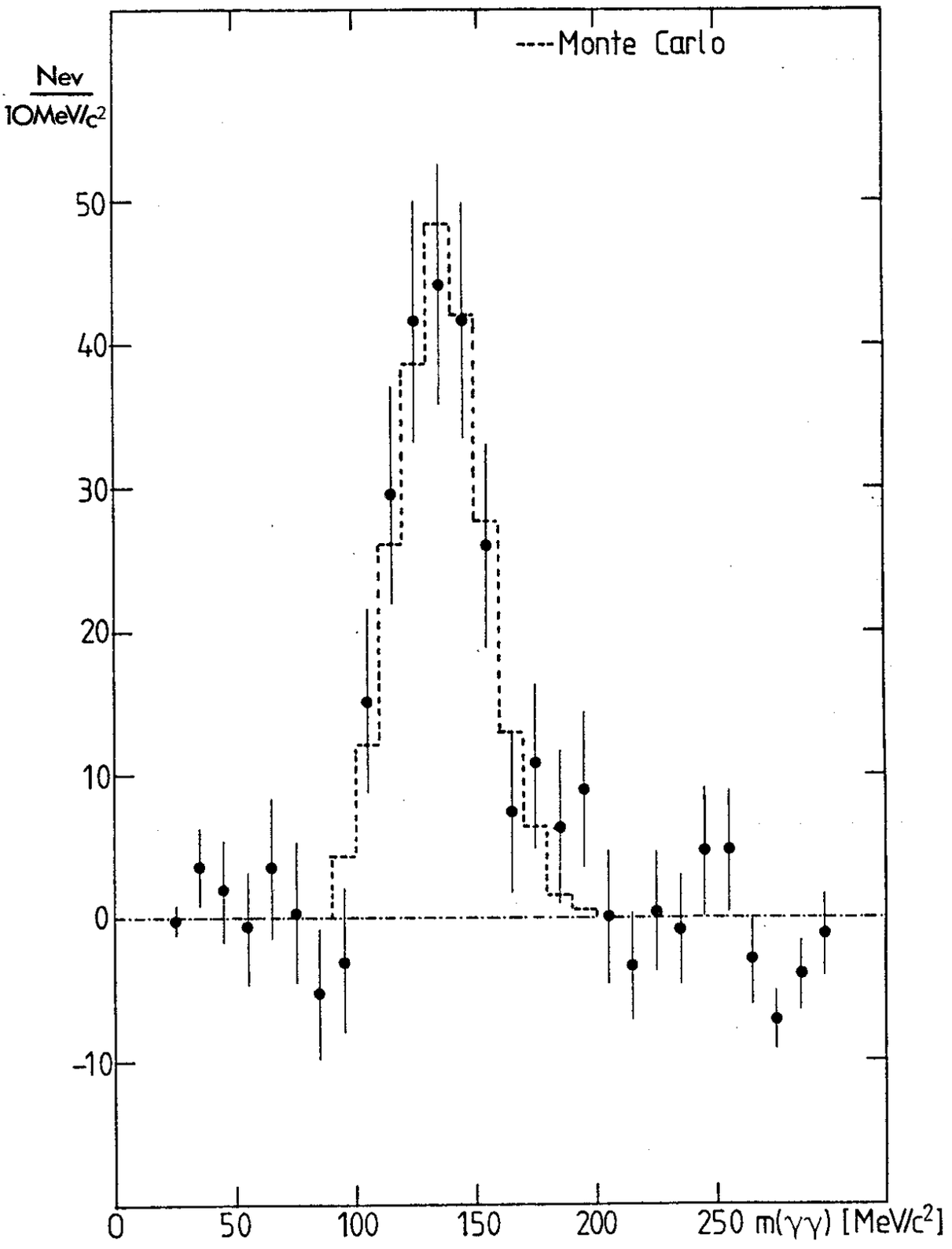
----Monte Carlo
Nev
10MeV/c²
50
40
30
20
10
0
-10
0
50
100
150
200
250 m(γγ) [MeV/c²]

Fig. 3

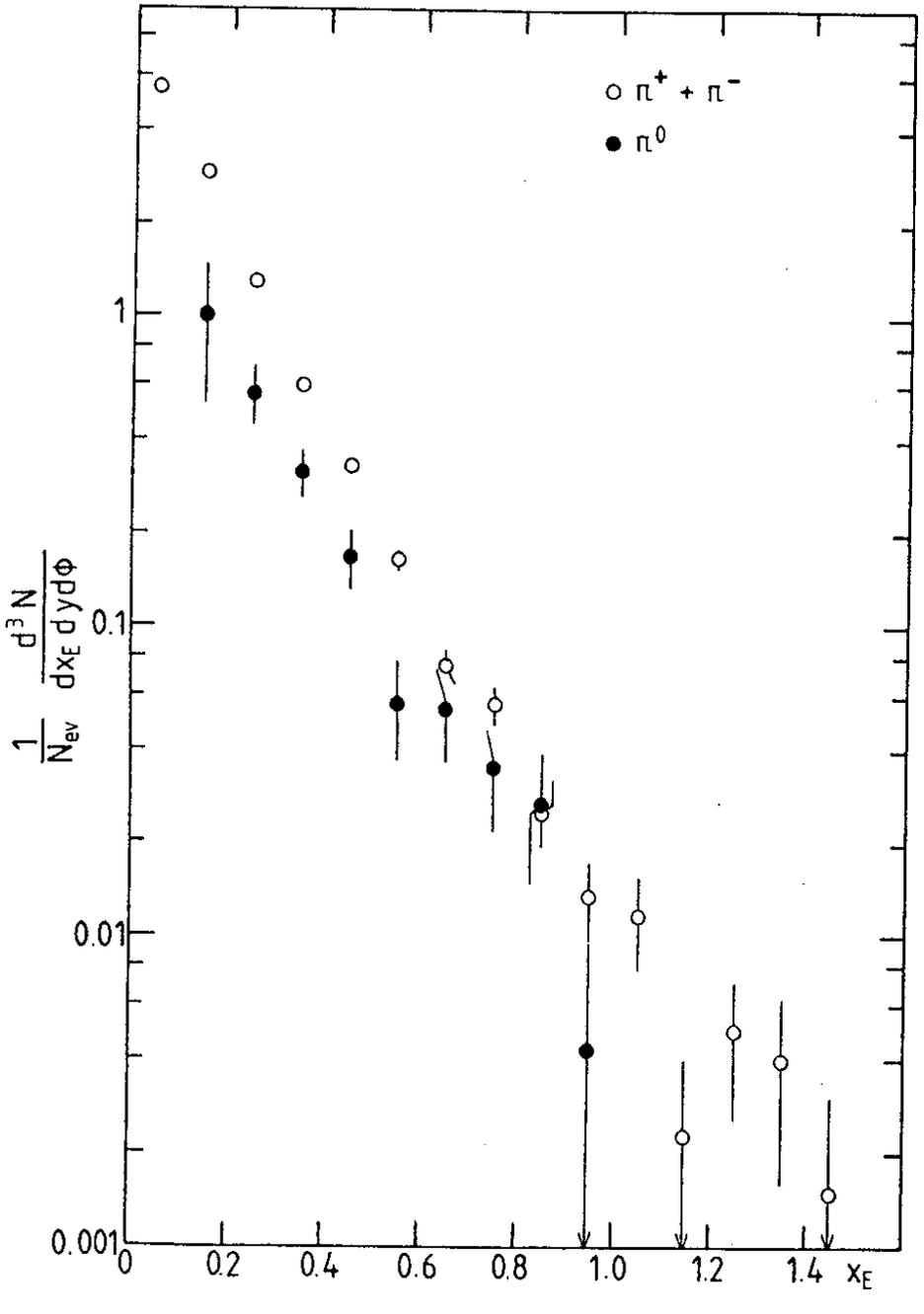
$\pi^+ + \pi^-$
π^0
$\frac{1}{N_{ev}} \frac{d^3N}{dx_E\, dy d\phi}$
1
0.1
0.01
0.001
0
0.2
0.4
0.6
0.8
1.0
1.2
1.4
x_E

Fig. 4a

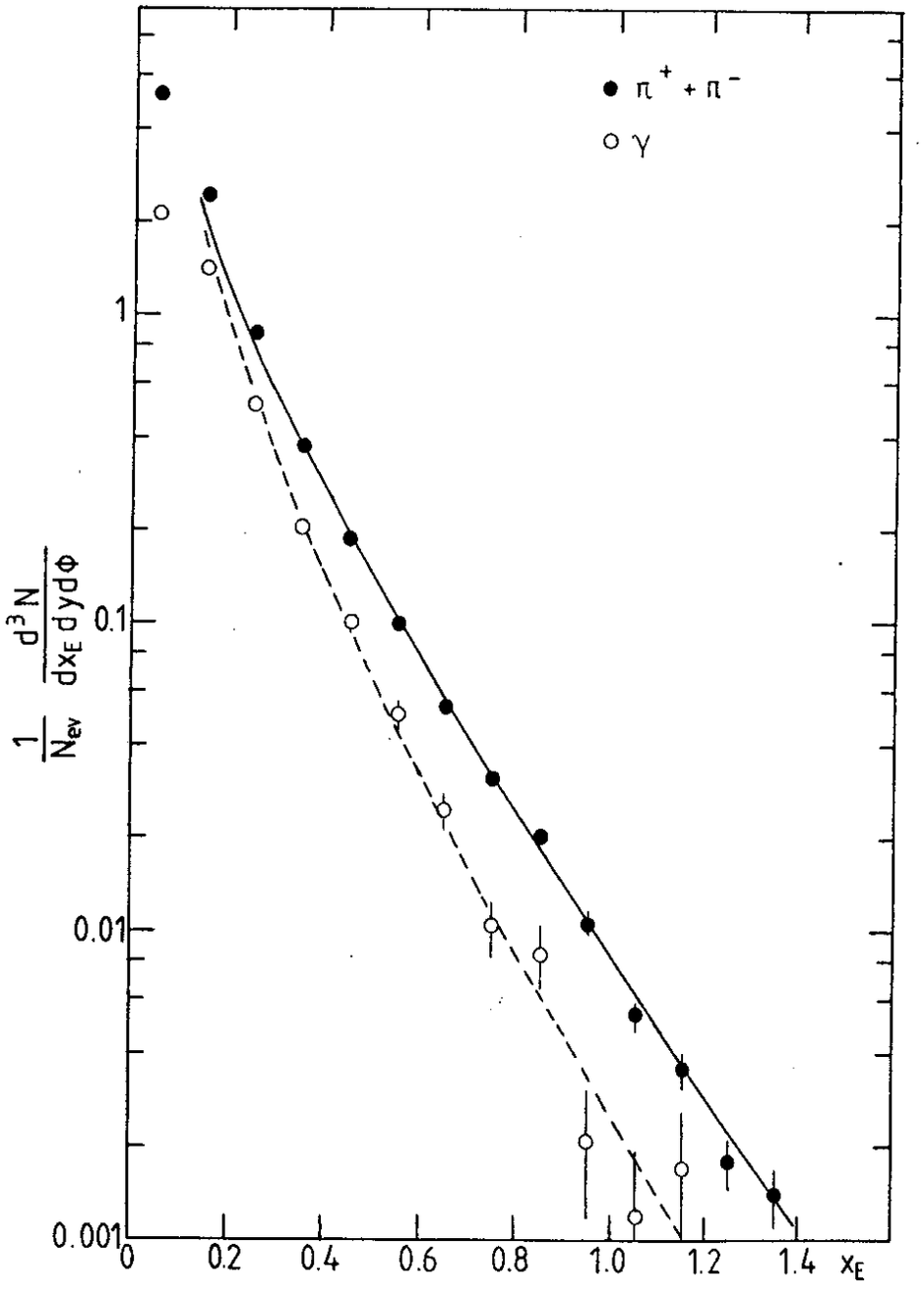
$\pi^+ + \pi^-$
γ
$\frac{1}{N_{ev}} \frac{d^3N}{dx_E\, dy d\phi}$
1
0.1
0.01
0.001
0
0.2
0.4
0.6
0.8
1.0
1.2
1.4
x_E

Fig. 4b